~~SECRET/RESTRICTED DATA~~

177 pgs.

Hydrodynamic and Nuclear Experiments (U)

Study Leaders:
R. J. Hemley
D. I. Meiron

Contributors:

H. Abarbanel
M. Adams
L. Bildsten
P. Dimotakis
S. Drell
D. Eardley
N. Fortson
R. Garwin
R. Jeanloz
J. Katz
R. Schwitters

November 2011

JSR-11-340

JSI-2011-027 Copy 0/6

Derived from: DD254, W15P7T-09-C-F402, Dated 1/23/09 and Multiple Sources.
Classifier: Robert Hanrahan, NNSA/DOE N121.1

~~RESTRICTED DATA~~
~~This attached document contains Restricted Data as defined in the Atomic Energy Act of 1954. Unauthorized disclosure subject to Administrative and Criminal Sanctions.~~

JASON
The MITRE Corporation
7515 Colshire Drive
McLean, Virginia 22102-7508
(703) 983-6997

~~SECRET/RESTRICTED DATA~~

~~SECRET/RD~~

REPORT DOCUMENTATION PAGE

Form Approved OMB No. 0704-0188

1. REPORT DATE *(DD-MM-YYYY)*	2. REPORT TYPE	3. DATES COVERED *(From - To)*
December 5, 2011	Technical	

4. TITLE AND SUBTITLE

Hydrodynamic and Nuclear Experiments (U)

5a. CONTRACT NUMBER

5b. GRANT NUMBER

5c. PROGRAM ELEMENT NUMBER

6. AUTHOR(S)

M. Adams, R. Schwitters, et al.

5d. PROJECT NUMBER

13109022

5e. TASK NUMBER

PS

5f. WORK UNIT NUMBER

7. PERFORMING ORGANIZATION NAME(S) AND ADDRESS(ES)

The MITRE Corporation
JASON Program Office
7515 Colshire Drive
McLean, Virginia 22102

8. PERFORMING ORGANIZATION REPORT NUMBER

JSR-11-340

9. SPONSORING / MONITORING AGENCY NAME(S) AND ADDRESS(ES)

U.S Department of Energy
1000 Independence Ave, SW
Washington D.C, 20585

10. SPONSOR/MONITOR'S ACRONYM(S)

11. SPONSOR/MONITOR'S REPORT NUMBER(S)

12. DISTRIBUTION / AVAILABILITY STATEMENT

Distribution authorized to US Government agencies only; Special Authority ODNI SEC S-08; Reason: 1.4(g); 27 January 2011. Other requests for this document shall be referred to DNI.

13. SUPPLEMENTARY NOTES

14. ABSTRACT

JASON was asked by the National Nuclear Security Administration (NNSA) to examine the current plans from the NNSA laboratories for hydrodynamic and subcritical experiments and to make recommendations for future efforts. The NNSA recently established the Office of Nuclear Experiments to coordinate a single long-term program of hydrodynamic experiments using surrogate materials and subcritical experiments using plutonium. The goal of this program is to develop improved understanding of the underlying physics of the materials and components in nuclear weapons in support of recent efforts such as the National Boost Initiative. JASON reviewed ongoing activities and plans for these experiments at the NNSA laboratories. The following summarizes the principal findings and recommendations of the report.

15. SUBJECT TERMS

16. SECURITY CLASSIFICATION OF:			17. LIMITATION OF ABSTRACT	18. NUMBER OF PAGES	19a. NAME OF RESPONSIBLE PERSON
a. REPORT	b. ABSTRACT	c. THIS PAGE			Dr. Robert Hanrahan
~~SECRET/RD~~	~~SECRET/RD~~	~~SECRET/RD~~	UL		19b. TELEPHONE NUMBER *(include area code)* 202-496-5156

Standard Form 298 (Rev. 8-98)
Prescribed by ANSI Std. Z39.18

~~SECRET~~

Meeting these challenges requires a continued effort to improve understanding of weapons performance for assessing the stockpile based on the quantification of margins and uncertainties (QMU). In conjunction with theory and simulation, a broad range of experiments supply relevant scientific and engineering data. Two kinds of data are obtained from such experiments, materials properties (particularly those of plutonium) and implosion characteristics for weapons-related geometries and materials in integrated systems. The requisite tools span a broad range of scales and costs, from bench-top instrumentation to large and complex facilities. This experimental program is executed at a variety of sites throughout the DOE complex. This effort is also informed by the large archival database provided by previous nuclear-explosion tests.

The program of hydrodynamic and nuclear experiments has several technical as well as programmatic objectives, and comprises a broad range of fundamental, focused, and integral experiments. Fundamental experiments include measurements of fundamental properties of materials, that is, intrinsic or atomic-level properties such as structures, phases, equations of state and other thermodynamic properties. Focused experiments include studies of non-equilibrium properties, as well as the behavior of real materials, and, in particular, weapons materials, with their defects, impurities, and microstructure; these can involve high-explosive-driven hydrodynamic experiments on plutonium in subcritical assemblies or on plutonium surrogates. Finally, integral experiments are conducted to assess the coupling of combinations of materials and may examine several operative phenomena simultaneously; they include large-scale hydrodynamic experiments as well as subcritical plutonium experiments, in weapons-relevant geometries.

The present study is motivated in part by a request to assess a program for a new series of integral experiments. These are subcritical implosion experiments on subscale primaries diagnosed via radiography or internal diagnostics compared with equivalent experiments on surrogate materials at full and subscale. The program is underway, and a plutonium subscale experiment is scheduled for execution in 2012.

3.4 Entropy Generation

Beyond the P-T-ρ EOS are thermochemical properties that determine equilibrium phase stability. During most of the course of a hydrodynamic experiment the flow is nearly isentropic. It is usually nearly adiabatic (except within detonating high

explosive or in nuclear explosions) because radiative and conductive heat flow and viscous dissipation are slow compared to hydrodynamic processes under "warm dense matter" conditions (temperatures of 0.1–10 eV, densities of 0.1–10 $\times$ solid density, and dimensions of tenths of mm or greater). The flow is therefore nearly isentropic except at shocks. In metals and covalently bonded solids, whose bulk moduli are generally $\mathcal{O}$(1 Mbar), shocks produced by high explosive are weak enough that the entropy change is usually small.

When entropy is nearly conserved in most of a flow, it is a powerful tool for thinking about the flow, and for numerical calculation. The choice of entropy as one of the independent thermodynamic variables is advantageous in reducing numerical errors. In calculation of processes that change all other variables by large factors the conservation of specific entropy is then automatic and explicit; it does not have to be enforced as an implicit constraint on the variation of two other independent variables, both of which vary by large amounts.

The use of entropy as an independent thermodynamic variable also facilitates understanding. When entropy is increased by some process, the effect of that process is immediately apparent. This would be less obvious when the variables are (for example) pressure and density, because then an increase in entropy appears as only a small (perhaps nearly invisible on a plot) shift of an element's trajectory in thermodynamic space. Sometimes small entropy differences may be important; they may determine the phase of a material, and many properties, including strength and the pressure-density relation, can be very different for two phases that are nearly in thermodynamic equilibrium.

The entropy of a substance is given by

$$S(T) = \int_0^T \frac{C_P(T')}{T'}\, dT', \tag{3}$$

where C_P is the heat capacity at constant pressure; we assume a thermodynamic path at constant (generally zero) pressure and a classical substance for which $S(0) = 0$. For an electron-degenerate metal, phonons contribute essentially all the specific heat,

which we describe by the Debye model (we ignore the more exotic excitations):

$$C_P(T) \approx \begin{cases} \frac{12\pi^4}{5}\left(\frac{T}{\Theta_D}\right)^3 nk_B & T < 0.234\ \Theta_D \\ 3nk_B & T > 0.234\ \Theta_D, \end{cases} \tag{4}$$

where the low temperature Debye approximation is taken for $T < 0.234\ \Theta_D$ and the un-quantized Dulong-Petit result for $T > 0.234\ \Theta_D$; the break point of $T = 0.234\ \Theta_D$ is chosen at the value of T at which these limiting forms are equal. In Equation 4, n is the ionic density and C_P is the specific heat per unit volume.

For $T > 0.234\ \Theta_D$

$$S(T) \approx 3k_B \left[\ln\left(\frac{T}{0.234\ \Theta_D}\right) + 0.004\right], \tag{5}$$

where $S(T)$ is the entropy per ion.

DOE (b)(3)

High explosive shocks in solids are fairly weak; their typical overpressures of 100–300 kbar are less (but not enormously less) than most solid condensed matter bulk moduli[4]. The entropy increase in an infinitesimal (acoustic) shock in a fluid is [22]

$$\Delta s = \frac{1}{12T_1}\left(\frac{\partial^2 V}{\partial P^2}\right)_s (\Delta P)^3, \tag{6}$$

where s is the entropy per gram, and must be multiplied by the atomic weight to get the entropy per ion (5), and V is the specific volume (the reciprocal of the density). The second partial derivative in Equation 6 is the first partial derivative of the compressibility (the reciprocal of the bulk modulus) with respect to pressure.

DOE (b)(3)

A figure of merit is the radius of the bore divided by the sample thickness. In a nominal experiment a shock (weak enough that its propagation speed is close to the sound speed in the shocked material) propagates through the thickness of the sample, and is reflected as an unloading rarefaction from a free surface normal to the shock and normal to the gun axis. If this figure of merit is two then the sample is completely unloaded from its periphery in the time required for the unloading wave from the free surface to penetrate its full depth. The minimal figure of merit for an experiment that only needs to study the loading wave, or the beginning of the unloading process, is unity. DOE (b)(3) DOE (b)(3) DOE (b)(3) The 40 mm bore powder gun provides this with margin to spare.

DOE (b)(3)

If the experiment includes a tamper or a fire-resistant shell. then the requirements may be more stringent. Sound speeds in most such materials are higher than in Pu (the thin rod sound speed is 5.1 km/s for stainless steel, 12.9 km/s for Be and 2.26 km/s for α-Pu). By itself, this imposes no further requirement on the bore diameter because both longitudinal and transverse loading and unloading occur at the same speed in each material. For example, a shock will traverse a steel tamper much faster than a plutonium shell, but neither the loading shock nor the release wave from its periphery will begin to enter the steel until it has passed through the plutonium. However, because of its lower density a tamper may be thicker than the plutonium. This is particularly so for Be, with density 1.85 (less than one tenth that of α-Pu).

4.4 Laser Platforms

As we have noted repeatedly above, there is a dearth of data to constrain the predictions of the dynamic behavior of Pu above 4-5 Mbar. Shown in Figure 23 is a notional path of Pu particle as the primary implodes. Note that constraints on the location

of phase boundaries as well as the location of the Hugoniot is only constrained by experiments up to pressures of 4-5 MBar. DOE (b)(3)

DOE (b)(3)

Gas gun facilities such as JASPER have been used to generate Hugoniot data up to about 5MBar and it has recently been possible to generate off-Hugoniot data in this regime as well. Beyond this regime it is necessary to use platforms such as Phoenix, NIF and Z. These facilities are important components of the 10 year DPE program plan.

We describe in this section the potential for Pu experiments on NIF to explore both the EOS and also investigate strength effects. The advantage of NIF will be the ultra-high pressures beyond 30 Mbar that can be reached. The idea is to tailor the laser drive so as to create ramp compressions that can either drive the target material onto the Hugoniot via shock compression or can be used to explore off-Hugoniot isentropes. Indeed it may be possible to use specially designed loadings to

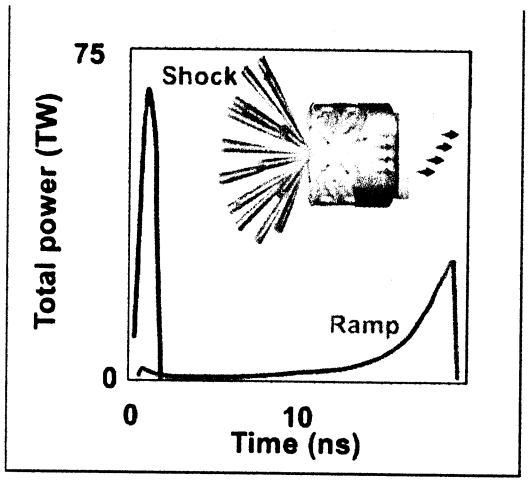

DOE (b)(3)

Figure 24: Left: the use of pulse shaping on NIF to produce either shock compression or ramp compression.

DOE (b)(3)

DOE (b)(3)

initially shock compress Pu and then drive it isentropically in a way similar to the environment experienced by a Pu particle in an imploding primary. The concept is shown graphically in Figure 24. Of course, the actual design of the appropriate pulse shape requires careful measurements but the initial experience with the NIF laser is encouraging. It has been repeatedly demonstrated that one can "program" a pulse of a given shape and the laser produces the desired pulse with impressive repeatability.

Questions have arisen regarding the accuracy of the measurements that will be achieved, and the extent to which ramp compression will be possible. For example it may not be possible to maintain isentropic compression at very high pressures without suffering formation of a shock in the material. This will require further investigation. On the other hand, the recent work on diamond to 50 Mbar and Ta to 6 Mbar is encouraging. In Figure 25 we show results from explorations of the Ta EOS on several platforms. The results shown correspond to isentropic compression As can be seen the new NIF data are in good agreement with previous data from the Omega laser and are also in agreement with data obtained on the Z pulsed power platform at SNL. The results are the highest pressure off-Hugoniot data achieved to date.

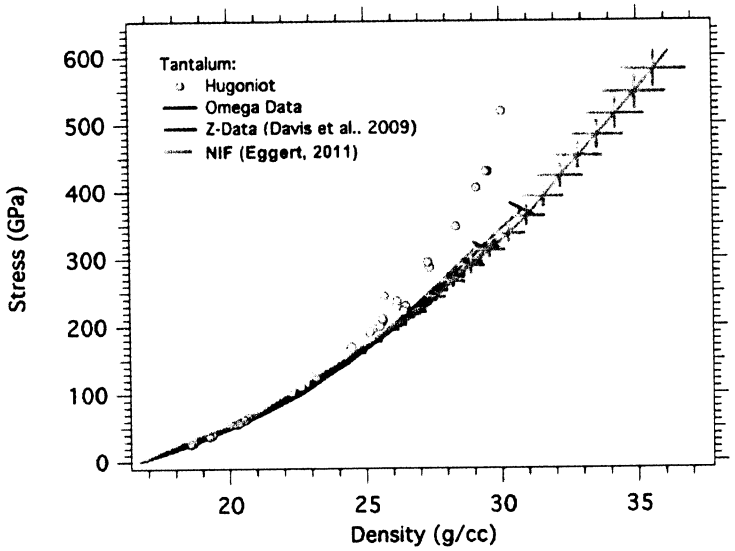

Figure 25: Measurements of the off-Hugoniot Ta EOS on several high pressure platforms.

No Pu experiments have yet been performed on NIF or Omega. Clearly this will require work to ensure that the appropriate safety issues can be addressed. Concerns have been voiced that the type of Pu that could be investigated is not weapons grade material which typically is alloyed with Ga, has various levels of impurities, and has differing isotopic compositions. In addition, it is likely that the microstructure of Pu samples on NIF also will not match that of weapons grade Pu used in primaries. However, in our view this is not a compelling objection. Indeed, from the point of view of fundamental measurements it is important to get a baseline on the pure material (both with and without Ga) as this high pressure data is very useful for informing theoretical approaches to characterize the more complex weapons grade material. Ultimately, of course, it will be be necessary to investigate the more complex weapons grade material and these issues will have to be addressed.

We next discuss the possible use of laser platforms in validating strength models at high pressure. Remington et al [54] have developed a laser-based platform to investigate various strength models. The basic idea is shown in Figure 26. A laser is aimed at a gold hohlraum which then produces X-rays that impinge upon an impactor which becomes a plasma after absorption of the X-ray flux. This plasma then

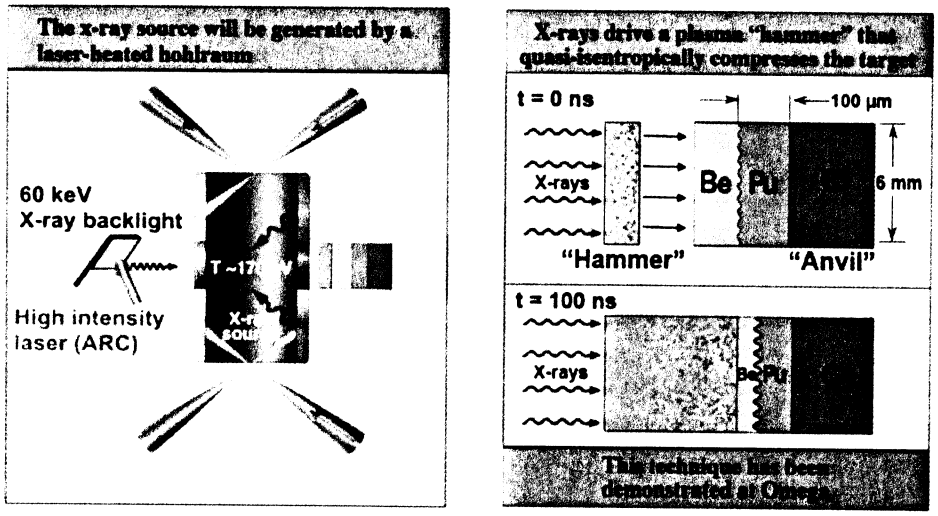

Figure 26: Laser platform for strength investigations

expands and transfers momentum to a target that creates a ramp-like compression on a layered target with a rippled interface. The interaction of the compression wave with the ripples interface produces baroclinically generated vorticity and thus an acceleration-induced instability known generically as Rayleigh-Taylor instability; that is, the rippled disturbance will grow at a rate that depends on the loading it receives but also on the nature of the materials across the interface. The growth rate in the absence of high pressure strength effects is different (larger) than that in the absence of such effects. Typical results are shown in Figure 27 where simulations of the instability both with and without strength are compared. Experiments of this type have been successfully carried out using high explosives at pRad as well as at the Omega laser and thus differing strain rates can be explored. With the advent of NIF even higher strain rates can be examined. The results have been used to validate various strength models. Shown in Figure 28 is the amplitude of the instability as a function of time for Ta as predicted by various strength models. Results are shown for material driven by HE loading as well as by laser drive on the Omega facility. As can be seen none of the current models in use for weapons simulation accurately predict the growth vs. time but of greater significance is the fact that the results are sensitive to the type of model used and this difference can be measured. Recently

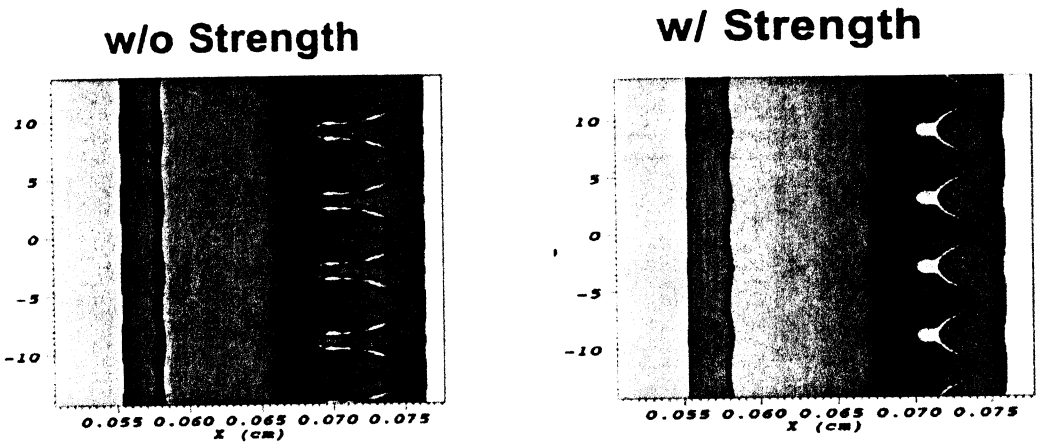

Figure 27: Comparison of strength effects on solid-solid Rayleigh-Taylor (R-T) instability.

Barton et al [34] have developed a multiscale strength model which attempts to model the mesoscopic processes such as dislocation dynamics. This model produces differing responses depending on the dislocation mobility.

Two experiments using R-T instability to infer strength on Ta have already been performed at NIF and more are scheduled. This will allow investigation of strength effects at upwards of 5 Mbar and will hopefully provide data which can further constrain strength models in use in weapons simulations. DOE (b)(3)

DOE (b)(3)

Overall, this type of approach holds promise for improving physics-based materials models for weapons materials that can be further validated in larger scale integrated experiments; however, the development of diagnostics with the requisite sensitivity and revolution will be challenging.

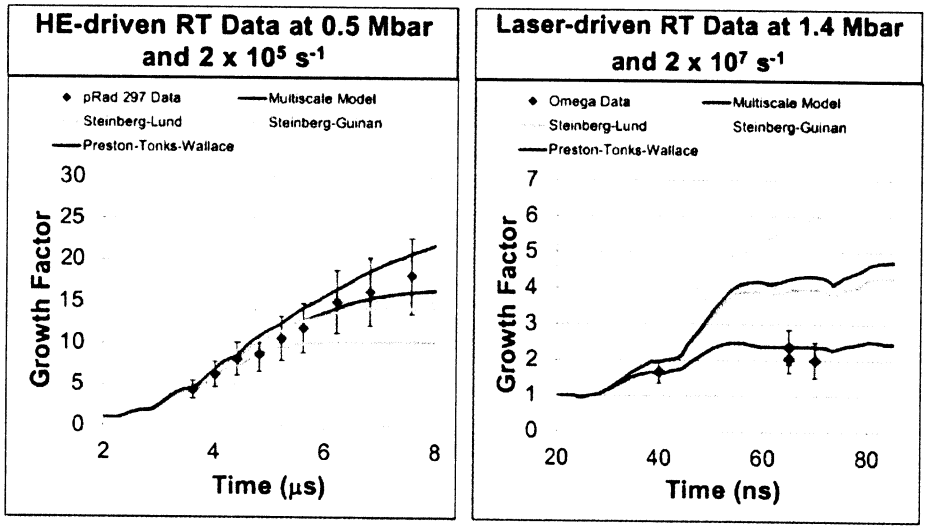

Figure 28: Growth rates for Rayleigh-Taylor (R-T) instability with strength effects. Loading is produced via high explosives (left) or the Omega laser (right). The predictions of various phenomenological models are also included as well as the prediction of a new multiscale model.

4.5 Pulsed Power

Pulsed power facilities provide the ability to examine materials under extreme P-T conditions and high strain rates of 10^5-10^6/sec, in principle in convergent or flat plate geometries. Because of the volume of material subjected to extreme conditions (linear dimensions of order 1 cm), multiple samples can be measured. The key facility for this work has been the Z machine at SNL, which was refurbished to increase its power by 50%. Z is now capable of both shock-wave compression to ~10 Mbar and ramp (*i.e.*, quasi-isentropic) compression to pressures of order 5 Mbar [55], generating the highest accuracy and precision data to date on materials at these conditions. DOE (b)(3)

DOE (b)(3)

Pulsed power can also be driven by high explosives (HEPP), and plans have been underway for several years for the construction of an HEPP facility at LLNL for this effort. This facility, called Phoenix, should could be complementary to that of Z with

the ability to reach higher pressures with longer dwell times (see Figure 4). As such, it would also have a niche for EOS measurements relative to NIF. However, no EOS data have yet been reported from this facility, and the viability of the diagnostics fielded at the facility has not been established and thus the accuracy of the data (*e.g.*, for the Pu EOS discussed above) cannot be assessed.

4.6 Static Compression

A broad range of static (and quasi-static) characterization experiments support the above hydrodynamic and nuclear experiments. These experiments include static compression methods such as those based on diamond anvil cells. The importance of these methods has been recognized since the inception the Stockpile Stewardship Program. They have provided the identification of the high P-T phases of Pu and Pu-Ga alloys, their phase boundaries and EOS to pressures of several megabars and temperatures of 2000–3000 K, as described above.

DOE (b)(3)

Static compression methods are readily can be combined with x-ray and neutron scattering and spectroscopy. Most recently, there have been important developments in examination of the development of texture and microstructure in situ at high P-T conditions using x-ray imaging methods. These imaging methods are useful for general characterization of materials recovered to ambient conditions as well.

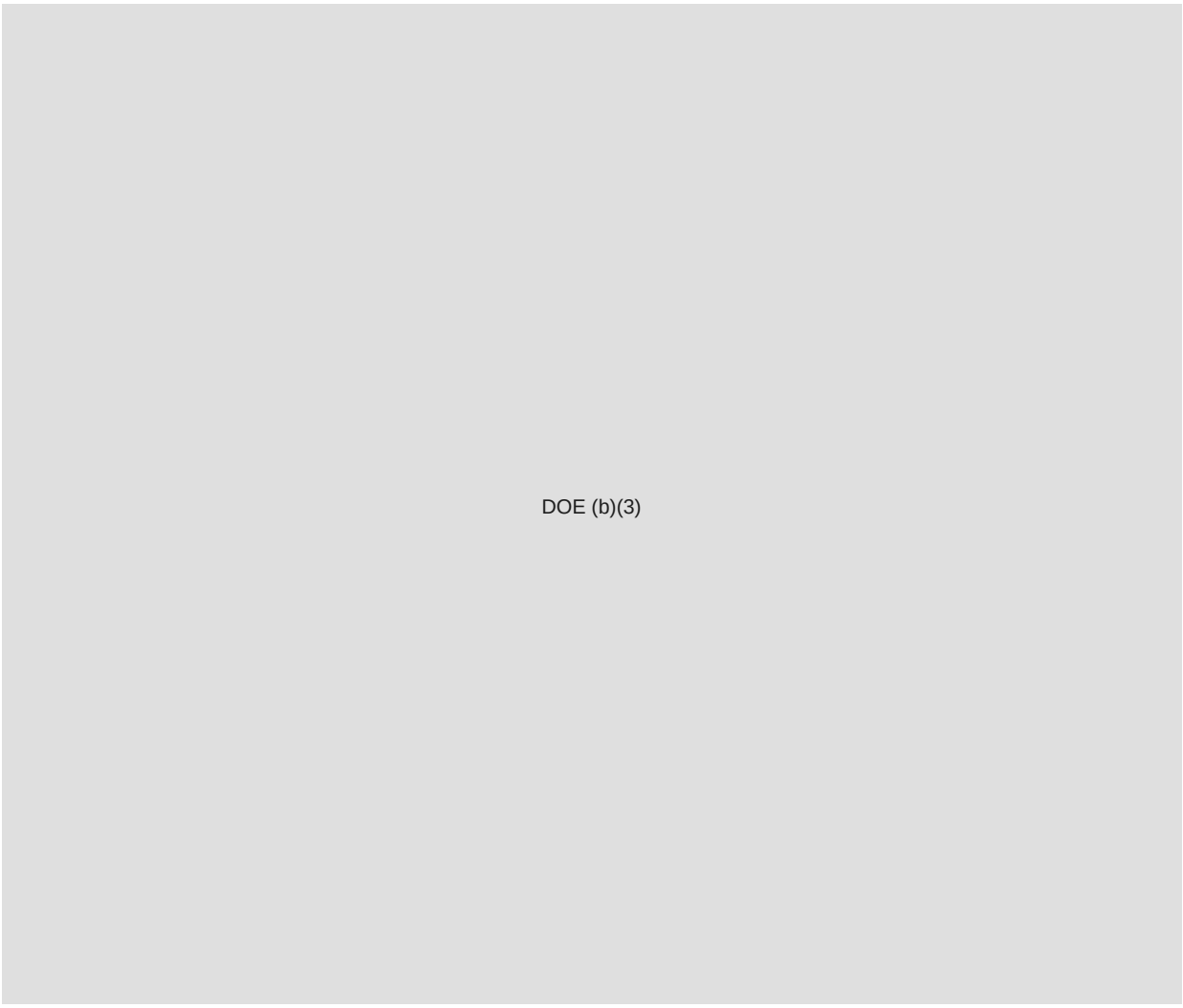

DOE
b(3)

5.2 Why Scaling (sort of) Works

Consider the motion of a continuum (either solid or fluid). In the Eulerian frame the equations of motion are

$$\begin{aligned} \frac{\partial \rho}{\partial t} + \frac{\partial (u_j \rho)}{\partial x_j} &= 0 \\ \frac{\partial \rho u_i}{\partial t} + \frac{\partial (u_j \rho u_i)}{\partial x_j} - \frac{\partial \sigma_{ij}}{\partial x_j} &= 0 \\ \frac{\partial E}{\partial t} + \frac{\partial (u_j E)}{\partial x_j} - \frac{\partial u_i \sigma_{ij}}{\partial x_j} &= 0 \end{aligned}$$

where ρ is the density, u_i is the velocity, σ_{ij} is the Cauchy stress tensor and

$$E = \frac{1}{2}\rho(u_i u_i) + \rho e$$

is the total energy density with e representing the internal energy per unit mass. All the physics is in the stress tensor.

If we scale lengths by some factor (call it β) and scale time by the same factor, that is

$$x_j \rightarrow \beta x_j \qquad t \rightarrow \beta t$$

it is not hard to see that the equations of motion are invariant with respect to this transformation provided

$$\sigma_{ij}(x_k, t) = \sigma_{ij}(\beta x_k, \beta t)$$

and, that the initial and boundary conditions are identical as well under the scaling transformation.

For the Euler equations for pure inviscid fluid motion we have

$$\sigma_{ij} = -P\delta_{ij},$$

where P is the thermodynamic pressure given by the equation of state. it can be seen that the equations are indeed scale free. For more complex constitutive relations scaling does not necessarily hold. Two important examples where scaling can fail to hold exactly come about when one uses rate dependent strength models or has a rate dependent energy release which may occur for certain reactive materials like high explosives. For example, if one uses a strength model to relate the stress tensor to strain and rate of strain, the strain tensor will in general not exactly scale. Similarly, the reaction zone of a high explosive may not scale properly and so the loading from the HE will modify the implosion so that it does not scale properly.

Scaling is also directly related to dimensional analysis and it can be shown that the presence of dimensionless quantities is directly related to measures of the violation of pure scaling. For example, the fact that viscous effects in fluids do not scale leads

to the development of the Reynolds number. Scaling or the lack thereof can be a powerful way to get insight into various physical effects and properly applied can be used to isolate and examine various effects separately. Indeed, an example of this is the fact that the contribution from fission energy becomes irrelevant provided the experiment is scaled so that the critical areal density is never reached during the implosion.

5.3 Scaled Implosions of a CHE Primary

DOE (b)(3)

probably making it impossible to distinguish propagated neutrons from the continuing source.

DOE (b)(3)

DOE (b)(3)

This latter factor would be larger in a nearly-critical assembly, and smaller in an assembly of non-fissionable (non-actinide) surrogate material.

DOE (b)(3)

Zippers are small electrostatic accelerators, used to initiate weapons and in oil well logging, generally producing 14.1 MeV neutrons by the D(T,n)α reaction. They must be placed outside the hydrodynamic experiment. Timing is at the choice of the experimenter, and it is possible to provide a number of pulses at suitable times, either by repeatedly firing one accelerator or by using several. The time of interest (usually that of central convergence) must be known in advance from hydrodynamic calculation; this has been done successfully for weapons for several decades and is not at issue. Neutron yields may be as large as 10^{10}.

Plasma Focus a company called Del Mar Ventures advertises its model ING-103 plasma focus neutron generator producing pulses of 10^{10} neutrons in a pulse width of 10–15 ns. Plasma focus machines, some with much larger neutron